

CHAPTER IV

CONCLUSIONS

Significant progress was made in this project in identifying the controlling factors in isosynthesis reactions with the objective of maximizing the production of isobutylene from zirconia based catalysts. First is the need to obtain an isosynthesis catalyst that is active at low temperatures so that the formation of methane can be minimized. Operation at 400 to 450 °C results in significant production of methane because of the hydrocracking of the higher alkanes produced at the higher conversions obtained in this study. Second is the identification and explicit statements of thermodynamic and kinetic limitations. When the C₅ olefins are the most thermodynamically favored product and the reaction is a series type reaction, there exists a kinetic and thermodynamic limit to the formation of isobutylene by the isosynthesis mechanism. Therefore, the horizons of the synthesis of isobutylene should be broadened to include isobutylene, isoamylene, and isohexene. These three compounds can also be used effectively to produce ethers for gasoline additives.

Catalysts prepared by the precipitation method show the most promise for future development as compared with those prepared hydrothermally, by calcining zirconyl nitrate, or by a modified sol-gel method. Precipitation is a comparatively simple procedure in which dopants can easily be added to the zirconia. For current catalysts the high temperatures (>673 K) required for activity also cause the production of methane (because of thermodynamics). A catalyst with higher activity at lower temperatures would magnify the unique selectivity of zirconia for isobutylene. Perhaps with a more active catalyst and acidification, oxygenate production could be limited at lower temperatures. Pressures above 50 atm cause an undesirable shift in product distribution toward heavier hydrocarbons.

Carbon deposition on the catalyst occurs fairly quickly (~2 hours) and does not alter the surface area compared with the deposition of heavier hydrocarbons. These hydrocarbons can be characterized as "soft coke" and are easily removed. A constant activity is reached within 4 hours after bringing a fresh catalyst on stream. Product distribution is more sensitive to changes in process conditions, especially temperature cycling.

Co-feeding hydrogen sulfide and presulfiding has the beneficial effect of decreasing C₂ and C₃ production while doubling or tripling C₅ production, especially 3-methyl-1-butene. Isobutylene fraction among the C₄'s also showed an increase. These changes in selectivity were accompanied by no loss in activity in the case of co-feeding and only a slight loss in the case of presulfiding. The resistance of zirconia to sulfur poisoning means that the sulfur in the synthesis gas (initially in the coal) need not be removed. The C₅ branched alkenes can be used to produce TAME which is also an additive currently being used in gasoline. The 3-methyl-1-butene can easily be isomerized into 2-methyl 2-(or 1-) butene since the branch needs to be located next to the double bond for TAME production. More study into the interaction between sulfur and zirconia would yield a better understanding of the selectivity change and possibly of the isosynthesis mechanism.

Oxygen vacancies are required for an active catalyst and may be responsible for the unique selectivity of isosynthesis catalysts. A catalyst doped with 1.72% Mg (wt) was the most active singly-doped zirconia with a CO conversion of 29% (32 wt% C₁, 29 wt% C₄, 26 wt% C₅+) at 673 K, 50 atm, 1/1 CO/H₂ ratio, and 90 second space time. A dopant that introduced the most oxygen vacancies per cation and was close in size to zirconium gave a more active catalyst. A multicomponent doped (Y-Ba-Cu) zirconia was more active but

produced more methane. Multiple dopings of zirconia may be the course needed to produce active catalysts at lower temperatures.

Catalyst characteristics have a strong impact on the stability and reactivity of the intermediates. Basic sites catalyze the CO insertions and acidic sites stabilize the methoxide species on the surface and promote condensation reactions. Both CO insertion and condensation reactions contribute to chain propagation in isosynthesis. A balance of acidity-basicity is important for an active isosynthesis catalyst. A deficiency of acidic sites or basic sites reduced the activity. However, strong acidity was not desirable since methane was produced from the excessive methoxide on the surface. Characterization of catalysts by temperature programmed desorption showed that acid-base properties were modified by preparation procedures. Zirconias prepared by the modified sol-gel method showed increased basicity as compared with those prepared by calcination of zirconyl salts.

A model was developed that can predict carbon monoxide conversion and product distribution. The rate equation for carbon monoxide conversion contains only a rate constant and an adsorption equilibrium constant. The product distribution was predicted using a simple ratio of the rate of CO conversion. No equations for predicting conversion or product distribution existed before this study. Additionally, the hydrocarbon distribution of isosynthesis was generated by a semi-empirical kinetic model with two adjustable parameters α and κ . The model was developed by adding an additional chain propagation step for C_2 intermediate to account for the contribution to chain growth by condensation reactions. The parameter α was defined as the probability of chain growth by CO insertion and κ was related to the ratio of condensation to CO insertion. Furthermore, desorption of β - C_3 intermediates was assumed to be negligible.

The form of the carbon monoxide rate equation can be obtained from three simplified mechanisms in which CO is either molecularly adsorbed or reacts from the gas phase, H_2 is dissociatively adsorbed, and CO_2 is the most strongly adsorbed/most abundant surface specie. Discrimination between these mechanisms was not possible. The values obtained by parameter estimation for activation energy and CO_2 heat of adsorption are reasonable. Analysis of the parameters obtained for modeling of the product distribution shows that the catalysts are most efficient in converting carbon from carbon monoxide into C_4 hydrocarbons. The model can be used for scale-up in the event isosynthesis becomes a more viable commercial process.

Nomenclature

a, b, c	exponent in empirical rate equation
d_i	rate constant for desorption
F	total molar flow rate in feed stock, mole/h
K_i	phase equilibrium constant for component i
K_{CO_2}	adsorption constant for CO_2 , atm^{-1}
k_i	rate constant for CO insertion
k_i'	rate constant for condensation
k_p	rate constant for CO production rate, $mole/(kg_{cat} atm^{1.5} s)$
n	number of carbon atoms in product
n_i	molar flow rate of component i , mol/hr
n_i^o	feed molar flow rate of component i , mol/hr
p_i^o, p_i	partial pressure of component i in the feed and at any point in the reactor.
P	total pressure, atm
P_i	mole fraction of hydrocarbons with carbon number i
R	gas constant, $atm cm^3 mol^{-1} K^{-1}$
r_i	reaction rate for component i
r_{CO}	reaction rate for CO, $mol/(sec kg_{cat})$
T, T_o	temperature and feed temperature, K
V, V_o	vapor molar flow rate of effluent and feed, mole/hr; catalyst volume, cm^3
W_{cat}	catalyst loading, kg
x	conversion
z_i	molar fraction for component i in the feed

Greek Symbols

α	probability of chain propagation
α_{ci}	number of carbon atoms for i th reaction
β	ratio of hydrogen to carbon monoxide in the feed
γ_j	rate constant ratio of component j to that of CO
γ_{ci}	rate constant ratio of component i to that of CO based on carbon
κ	ratio of condensation to propagation
ρ_b	catalyst bulk density, g/cm^3
σ_j	reaction extent for reaction j
τ	space time, sec
v_o	inlet volumetric flow rate, cm^3/sec
ψ_i	amount reacted or produced by reactions for component i

REFERENCES

1. Hoffman, H., *Hydrocarbon Process.* **69**, 15 (1990).
2. Piel, W.J., and Thomas, R.X., *Hydrocarbon Process.* **69**, 68 (1990).
3. Ainsworth, S.J., *Chem. Engr. News* **69**, 13 (1991).
4. Sofianos, A., *Catal. Today* **15**, 149 (1992).
5. Johnson, J.E., and Peterson, F.M., *CHEMTECH* **21**, 296 (1991).
6. Nakamura, D.W., *Hydrocarbon Process.* **72**, 21 (1993).
7. Pichler, H., and Ziesecke, K., *Brennst. Chem.* **30**, 1 (1949).
8. Kieffer, R., Varela, J., and Deluzarche, A., *J. Chem. Soc. Chem. Commun.* 763 (1983).
9. Maehashi, T., Maruya, K., Domen, K., Aika, K., and Onishi, T., *Chem. Lett.* 747 (1984).
10. Maruya, K., Maehashi, T., Haraoka, T., Narui, S., Asakawa, Y., Domen, K., and Onishi, T., *Bull. Chem. Soc. Jpn.* **61**, 667 (1988).
11. Maruya, K., Fujisawa, T., Takasawa, A., Domen, K., and Onishi, T., *Bull. Chem. Soc. Jpn.* **68**, 11 (1989).
12. Tseng, S.C., Jackson, N.B., and Ekerdt, J.G., *J. Catal.* **109**, 284 (1988).
13. Jackson, N.B., and Ekerdt, J.G., *J. Catal.* **126**, 31 (1990).
14. Jackson, N.B., and Ekerdt, J.G., *J. Catal.* **126**, 46 (1990).
15. Mazanec, T.J., *J. Catal.* **98**, 115 (1986).
16. Davis, B., *J. Am. Ceram. Soc. Comm.* **67**, C-168 (1984).
17. Srinivasan, R., De Angelis, R., and Davis, B.H., *J. Mater. Res.* **1**, 583 (1986).
18. Li-Min, T., Srinivasan, R., De Angelis, R.J., Pinder, T., and Davis, B.H., *J. Mater. Res.* **3**, 561 (1988).
19. Benedetti, A., Fagherazzi, G., and Pinna, F., *J. Am. Ceram. Soc.* **72**, 467 (1989).
20. Benedetti, A., Fagherazzi, G., Pinna, F., and Polizzi, S., *J. Mater. Sci.* **25**, 1473.

(1990).

21. Smith, D.K., and Newkirk, H.W., *Acta. Cryst.* 18, 983 (1965).
22. Jansen, H.J.F., *Phys. Rev. B* 43, 7267 (1991).
23. Bragg, L., and Claringbull, G.F., in "The Crystalline State" (L. Bragg, Ed.), Vol. IV-Crystal Structures of Minerals, p. 239. Cornell University Press, New York, 1965.
24. Stull, D.R., Westrum, E.F. Jr., and Sinke, G.C., "The Chemical Thermodynamics of Organic Compounds," Wiley & Sons, New York, 1969.
25. Fajula, F., Anthony, R.G., and Lunsford, J.H., *J. Catal.* 73, 237 (1982).
26. Gadalla, A.M., Chan, T., and Anthony, R.G., *Inter. J. Chem. Kinet.* 15, 759 (1983).
27. Dry, M.E., in "Catalysis. Science and Technology" (J.R. Anderson and M. Boudart, Eds.), Vol. I, Springer-Verlag, New York, New York, 1980.
28. Anderson, R.B., in "Catalysis" (P.H. Emmett, Ed.), Vol. IV, Reinhold, New York, New York, 1956.
29. Hofer, L.J.E., in "Catalysis" (P.H. Emmett, Ed.), Vol. IV, Reinhold, New York, New York, 1956.
30. Snel, R., *Catal. Rev.-Sci. Eng.* 29, 361 (1987).
31. Aris, R., "Elementary Chemical Reactor Analysis," Prentice Hall, Englewood Cliffs, New Jersey, 1969.
32. Holland, C.D., and Anthony, R.G., "Fundamentals of Chemical Reaction Engineering," Prentice Hall, Englewood Cliffs, New Jersey, 1989.
33. Rabo, J.A., Risch, A.P., and Poutsma, M.L., *J. Catal.* 53, 295 (1978).
34. Karles, G.D., and Ekerdt, J.G., Preprint Paper-Amer. Chem. Soc., Div. Petr. Chem., Inc. 37, 239 (1992).
35. Evans, P.A., Stevens, R., and Binner, J.G.P., *Br. Ceram Trans. J.* 83, 39 (1984).
36. Dosch, R.G., Stephens, H.P., and Stohl, F.V., U.S. Patent 4,511,455 (1985).
37. "Powder Diffraction File," Alphabetical Index, Compiled by the JCPDS - International Centre for Diffraction Data, Swarthmore, PA, 1987.

38. Jackson, N.B., Ph.D. Dissertation, Department of Chemical Engineering, University of Texas, Austin, Texas, 1990.
39. Kieffer, E.P., and Van Der Baan, H.S., in "Chemical Reaction Engineering" (M.J. Comstock, Ed.), ACS Symposium Series No. 196, 1981.
40. Henderson, A.W., and Higbie, K.B., *J. Am. Chem. Soc.* **76**, 5878 (1954).
41. Barker, M.A., M.S. Thesis, Department of Chemical Engineering, University of Texas, Austin, Texas, 1987.
42. Saryp, B., and Wojciechowski, B.W., *Can. J. Chem. Eng.* **66**, 831 (1988).
43. Dean, J.A. Ed., "Lange's Handbook of Chemistry" 13th edition, McGraw-Hill Book Company, New York, p.3-121 - 3-126 (1985).
44. Mackrodt, W.C., and Woodrow, P.M., *J. Am. Ceram. Soc.* **69**, 277 (1986).
45. Rajendran, S., Swain, M.V., and Rossell, H.J., *J. Mater. Sci.* **23**, 1805 (1988).
46. Rajendran, S., Drennan, J., and Badwal, S.P.S., *J. Mater. Sci. Lett.* **6**, 1431 (1987).
47. Silver, R.G., Hou, C.J., and Ekerdt, J.G., *J. Catal.* **118**, 400 (1989).
48. Platero, E.E., and Mentruit, M.P., *Mater. Lett.* **14**, 318 (1992).
49. Nakajo, T., Arakawa, H., Sano, K.-I., and Matsuhira, S., *Chem. Lett.* 593 (1987).
50. Etsell, T.H., and Flengas, S.N., *Chem. Rev.* **70**, 339 (1970).
51. Jackson, N.B., and Ekerdt, J.G., *J. Catal.* **101**, 90 (1986).
52. Uehara, T., Koto, K., Emura, S., and Kanamaru, F., *Solid State Ionics* **23**, 331 (1987).
53. Strickler, D.W., and Carlson, W.G., *J. Am. Ceram. Soc.* **48**, 286 (1965).
54. Badwal, S.P.S., and Drennan, J., *Solid State Ionics* **53-56**, 769 (1992).
55. Gur, T.M., Raistrick, I.D., and Huggins, R.A., *Mater. Sci. Engr.* **46**, 53 (1980).
56. Kaneko, H., Jin, F., Taimatsu, H., and Kusakabe, H., *J. Am. Ceram. Soc.* **76**, 793 (1993).
57. Stafford, R.J., Rothman, S.J., and Routbort, J.L., *Solid State Ionics* **37**, 67 (1989).

58. Smith, J.M., "Chemical Engineering Kinetics," 3rd ed., McGraw-Hill, New York 1981.
59. Calderbank, P.H., and Moo-Young, M.B., *Chem. Engr. Sci.* **16**, 39 (1961).
60. Brian, P.L.T., Hales, H.B., and Sherwood, T.K., *AIChE J.* **15**, 419 (1969).
61. Yokoyama, A., Komiyama, H., Inoue, H., Masumoto, T., and Kimura, H., in "Chemical Reaction Engineering" (M.J. Comstock, Ed.), ACS Symposium Series No. 196, 1981.
62. Izarraraz, A.G., Benzen, G.W., Anthony, R.G., and Holland, C.D., *Hydrocarbon Process.* April, (1980).
63. Graaf, H., Smit, H.J., Stamhuls, E.J., and Beenackers, A.A.C.M., *J. Chem. Eng. Data* **37**, 146 (1992).
64. Norris, J.C., "Engineering Data Book," 9th ed., Gas Processors Association, Tulsa, OK, 1972.
65. Lee, H.H., "Heterogeneous Reactor Design," Butterworth Publishers, Boston, 1985.
66. Saryp, B., and Wojciechowski, B.W., *Can. J. Chem. Eng.* **67**, 62 (1989).
67. Lamotte, J., Lavalley, J.C., Druett, E., and Freund, E., *J. Chem. Soc. Faraday Trans. 1* **79**, 2219 (1983).
68. He, M.Y., and Ekerdt, J.G., *J. Catal.* **87**, 381 (1984).
69. Frolich, P.K., and Cryder, D.S., *I & EC Chem.* **22**, 1051 (1930).
70. Smith, K.J., and Anderson, R.B., *J. Catal.* **85**, 428 (1984).
71. Boudart, M., *AIChE J.* **18**, 465 (1972).

APPENDIX A - Relationship Between wt% and Carbon Conversion

Relationship Between wt% and Carbon Conversion

The total carbon conversion is equivalent to the total carbon monoxide conversion. From the stoichiometry of the reactions to produce alkanes and alkenes it can be shown that half of the carbon monoxide reacted is converted to carbon dioxide. The carbon converted to each of the hydrocarbon groups C_i is given by

$$x_{C-C_i} = \frac{\text{moles of carbon in } C_i}{\text{total moles of carbon converted to hydrocarbons}} \quad (\text{A.1})$$

this becomes

$$x_{C-C_i} = \frac{2 \alpha_{C_i} y_{C_i} n_T}{y_{CO}^o n_T^o - y_{CO} n_T} \quad (\text{A.2})$$

The α_{C_i} 's are the number of carbons in each product. The relationship between $y_{C_i} n_T$ and weight fraction, w_i , (wt fraction equals wt percent divided by 100) is given by

$$y_{C_i} n_T = \frac{w_i TG_{HC}}{MW_i} \quad (\text{A.3})$$

TG_{HC} is the total grams of hydrocarbons produced per hour (when molar flow rate is mol/hr). When this is substituted into equation (A.2) the result is

$$x_{C-C_i} = \frac{2 \alpha_{C_i} TG_{HC} w_i}{MW_i (y_{CO}^o n_T^o - y_{CO} n_T)} \quad (\text{A.4})$$

The results for carbon conversion are normalized if the total is not exactly 100. The error introduced by assuming an average molecular weight for C_2 , C_3 , C_4 , and C_5+ fractions is small since usually the difference is only two hydrogen atoms. An example of this calculation is given in Table A.1 for a run over the 7% Ce-ZrO₂ catalyst.

TABLE A.1. Comparison of wt% with carbon conversion to that hydrocarbon group for run C7B (673K, 50 atm, 1/1 CO/H₂ ratio, and 60 second space time)

Hydrocarbon group	wt%	Carbon conversion (%)
C ₁	29.46	27.18
C ₂	8.29	8.44
C ₃	7.05	7.26
C ₄	29.00	30.24
C ₅ +	26.21	26.88

APPENDIX B - Rate Equation Parameters, Surface Intermediates, and Simplified Mechanisms

This appendix contains some discussion about the physical meaning of the parameters obtained for the carbon monoxide rate equation, mechanisms describing the surface intermediates involved in the isosynthesis, and some possible simplified mechanisms that could account for the final form of the rate equation.

Parameters in the Carbon Monoxide Rate Equation

Recall that an equivalent fit of the data was obtained using the following equation with $a=1$, $b=0.5$, and $c=1$ or 2 . The expression with $c=1$ was used for modeling in this study because it was the simpler equation.

$$r_{CO} = \frac{k_p p_{CO}^a p_{H_2}^b}{(1 + K_{CO_2} p_{CO_2})^c} \quad (B.1)$$

The values obtained for a and b indicate that carbon monoxide was adsorbed as a molecule, while hydrogen was dissociatively adsorbed. Table B.1 shows the comparison of fitted parameters for the cases where c either equals 1 or 2. This example is for the 7% Ce-ZrO₂ while co-feeding hydrogen sulfide and using the aluminum carbon monoxide cylinder. Both the rate constant and adsorption equilibrium constant are affected by the change in c value, though the effect is more significant for the adsorption equilibrium constant. Table B.2 shows the change in calculated activation energy and CO₂ heat of adsorption for the two models using the SimuSolv[®] parameters in Table B.1.

The change in activation energy is within the experimental error, while the change in CO₂ heat of adsorption is about 12%. Lee (65) gave two rules that can be used to test the significance of adsorption equilibrium constants that appear in Langmuir-Hinshelwood expressions. These rules are given by the following equations.

$$10 < (-\Delta S_a)^\circ < 12.2 - 0.0014(\Delta H_a)^\circ \quad (B.2)$$

$$0 < (-\Delta S_a)^\circ < (S_g)^\circ \quad (B.3)$$

Where $(\Delta S_a)^\circ$ (*cal/mol K*) is the entropy change referred to a standard state of 1 atm at the temperature of adsorption, $(\Delta H_a)^\circ$ (*cal/mol*) is the corresponding enthalpy change, and $(S_g)^\circ$ is the standard state entropy of the gas phase. Stull *et al.* (24) give $(S_g)^\circ$ as 59.9 *cal/mol K* for CO₂ at 700 K. The entropy change and enthalpy change can be found from the following equation:

$$K_{CO_2} = e^{(\Delta S_a)^\circ/R} e^{-(\Delta H_a)^\circ/RT} = A e^{\lambda/RT} \quad (B.4)$$

The value of $(\Delta S_a)^\circ$ is found from the y-intercept of the plot to find $(\Delta H_a)^\circ$. Using the two $-(\Delta H_a)^\circ$ values calculated for c equal to either 1 or 2, Equation (B.2) can be reduced to

$$10 < (-\Delta S_a)^\circ < 32 \quad (\text{cal/mol K}) \quad (B.5)$$

and

$$10 < (-\Delta S_a)^\circ < 30 \quad (\text{cal/mol K}) \quad (\text{B.6})$$

for the cases of $c=1$ and $c=2$ respectively. The calculated $(\Delta S_a)^\circ$ values are -22.43 cal/mol K and -21.35 cal/mol K respectively. These entropy values satisfy Equations (B.5) and (B.6) respectively and also satisfy the requirement of Equation (B.3). This result, combined with the fact that the adsorption equilibrium constant for CO_2 (found in this study) decreases with increasing temperature indicates that this is a true equilibrium constant and not a ratio of rate constants. Similar results are obtained for the other catalysts for which activation energies and heats of adsorption for CO_2 were calculated. In this study, the difference in fit between $c=1$ and $c=2$ was not significant enough to reject one of the models. Therefore the simpler equation ($c=1$) was utilized.

Surface Intermediates

Modification of catalyst properties affects the isosynthesis activity, as shown in the previous sections. There are similarities between the mechanism of isosynthesis and that of Fischer-Tropsch synthesis. Hydrocarbons are formed in both processes by chain reactions starting with C_1 intermediates (15,27-29,42,66), and the chain reactions include chain initiation, chain growth, and chain termination. However, the products from isosynthesis are rich in branched hydrocarbons, whereas F-T synthesis yields primarily linear products. Furthermore, the product distribution of isosynthesis does not resemble an Anderson-Schulz-Flory distribution. Therefore, a different mechanism is needed for isosynthesis. The mechanisms of isosynthesis and the interactions between surface intermediates and acidic and basic sites are discussed in the following sections.

Chain initiation

The first step of isosynthesis, as in any other synthesis gas reactions, is the activation of CO and H_2 on the surface. Hydrogen has been shown to undergo heterolytic cleavage on ThO_2 (67), which is an active isosynthesis catalyst. The adsorption of CO on an isosynthesis metal oxide is non-dissociative, which is different with that on the F-T catalyst in which CO is dissociatively adsorbed (15).

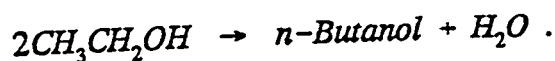
Coadsorption of carbon monoxide and hydrogen produces adsorbed formaldehyde (I) and methoxide (II) species on the surface (8,11,15,38,68), as shown in Figure B.1. Anion vacancies (i.e., oxygen vacancies for zirconia) are believed to be active sites for the formation of methoxide (15,38,47,51). The C_1 species will undergo a series of reaction to form hydrocarbons.

Chain propagation

CO insertion is the primary carbon-carbon bond-forming step (15). The first step in the CO insertion is the formation of a cyclic acyl (III). Then, the cyclic acyl is hydrogenated to form a coordinated diol (IV), which can be rearranged to an enol (V) and dehydrated to an adsorbed aldehyde (VI), as shown in Figure B.2. CO insertion is similar to the chain growth in F-T synthesis.

The condensation reaction is another mechanism for chain-propagation. The name

was first proposed by Frolich and Cryder (69) to describe the formation of higher alcohols from lower alcohols, such as :



More recently, Smith and Anderson (70) studied the distribution of higher alcohols over promoted methanol synthesis catalyst, and proposed a scheme in which one- or two-carbon species can add to the growing intermediates to give higher products. The chain growth can be at the α or β carbon atom, and β addition accounts for the selectivity to branched products.

In isosynthesis, condensation is faster for the C_2 species than for the C_3 and C_4 species (8,12,15). The reaction involves alkylation by a nearby alkoxide (primarily methoxide because of its large surface concentration) of an η^3 -enolate (VII) at the terminal carbon atom to form an adsorbed aldehyde (VIII in Figure B.3). The condensation reactions are slow compared with CO insertion reactions, but are kinetically significant due to the large surface concentration of methoxide groups on the surface (15).

The condensation reaction as a unique chain growth mechanism for isosynthesis, provides an additional route for chain propagation other than CO insertion, and is the primary factor that causes the deviation of product distribution of isosynthesis from the Anderson-Schulz-Flory distribution for a standard polymerization reaction.

Formation of branched products

Unlike Fischer-Tropsch synthesis, isosynthesis produces branched hydrocarbons. Mazanec (15) contributed the formation of branched products to two different enols (X and XIII in Figure B.4) from a coordinated 1,2-propanediolate (IX). These two routes lead to two different types of η^3 -enolates (XI and XIV), and eventually to linear (XII) and branched (XV) adsorbed aldehydes. Both η^3 -enolates are stabilized on oxides such as ZrO_2 and ThO_2 (15), which contributes to the selectivity of branched products on these metal oxides.

The mechanism described herein provides information on how the intermediates are formed and reacted. The nature of the catalyst surface has a strong impact on the relative stability of these intermediates and precursors, which ultimately determines the distribution of products.

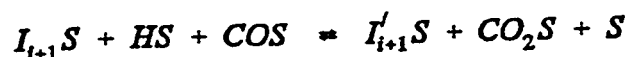
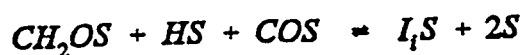
Simplified Mechanisms

In this section three mechanisms will be discussed that, with simplifying assumptions, lead to the final form of the rate equation found by the empirical fit. Boudart (71) used two simplifying assumptions to reduce complex Langmuir-Hinshelwood expressions. These assumptions were: (1) one step is the rate-determining step, and (2) one surface intermediate is dominant and thus all the other intermediates are present in relatively insignificant amounts. Using these assumptions it is not necessary to assume details of the overall mechanism.

CO and H₂ adsorbed, single catalyst site

In this mechanism CO is molecularly adsorbed and H₂ is dissociatively adsorbed on

the same type of catalyst site and react to form intermediates on the surface according to the following eight steps.



In this notation S is a surface catalyst site, I_i ($i \geq 2$) is a surface intermediate with the structure $C_i H_{2i-1} O_2$, and I'_i ($i \geq 2$) is a surface intermediate with the structure $C_i H_{2i} O$. These propagation steps can continue on the surface, or the intermediates can desorb to form products as shown in the following two steps.



This mechanism is written so alkenes are formed, therefore P_i ($i \geq 2$) has the structure $C_i H_{2i}$; however, similar steps could be written for alkane formation. If the third step is taken to be rate controlling and essentially irreversible then the carbon monoxide rate equation can be written as follows.

$$r_{CO} = k_3 c_{COS} c_{HS} \quad (B.7)$$

The concentrations of molecular carbon monoxide and atomic hydrogen on the catalyst surface can be solved for using the first two steps of the mechanism.

$$c_{COS} = K_{CO} P_{CO} c_S \quad (B.8)$$

$$c_{HS} = \sqrt{K_{H_2} P_{H_2}} c_S \quad (B.9)$$

The adsorption equilibrium constant for CO and H_2 are defined as the ratio of the rate constant for adsorption divided by the rate constant for desorption. When Equations (B.8) and (B.9) are substituted into Equation (B.7) the following equation results.

$$r_{CO} = k_3 K_{CO} \sqrt{K_{H_2}} p_{CO} p_{H_2}^{0.5} c_S^2 \quad (\text{B.10})$$

The concentration of surface sites (c_S) can be solved for by using a total site balance.

$$c_T = c_S + c_{COS} + c_{HS} + c_{CHOS} + c_{CH_2OS} + \sum_{i=2}^n c_{I_i S} + \sum_{i=2}^n c_{I'_i S} + c_{CO_2 S} \quad (\text{B.11})$$

If carbon dioxide is assumed to be the most abundant surface intermediate, since more of this specie is formed than any other intermediate, then the total site balance can be reduced to the following expression.

$$c_T = c_S + K_{CO_2} p_{CO_2} c_S \quad (\text{B.12})$$

The adsorption equilibrium constant for carbon dioxide is defined in the same manner as those for carbon monoxide and hydrogen. When Equation (B.12) is solved for c_S and substituted into Equation (B.10) the result is

$$r_{CO} = \frac{k_p p_{CO} p_{H_2}^{0.5}}{(1 + K_{CO_2} p_{CO_2})^2} \quad (\text{B.13})$$

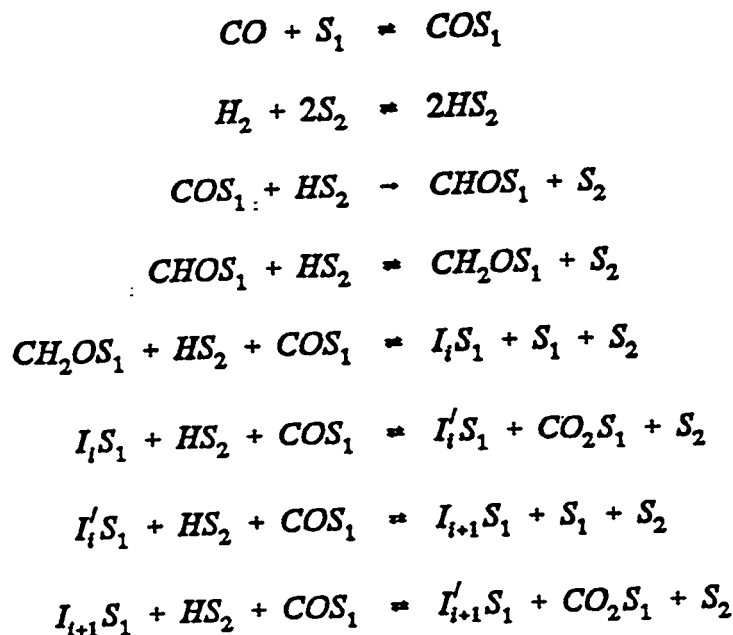
where

$$k_p = k_3 K_{CO} \sqrt{K_{H_2}} c_T^2 \quad (\text{B.14})$$

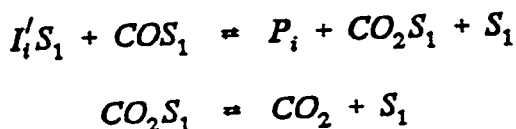
This mechanism leads to a final expression in which the denominator is squared ($c=2$ from empirical fit).

CO and H₂ adsorbed, dual catalyst sites

In this mechanism CO is molecularly adsorbed and H₂ is dissociatively adsorbed on different types of catalyst sites and react to form intermediates on the surface according to the following eight steps.



In this case, S_1 and S_2 are the two types of surface catalyst sites. The other notation is the same as previously given. The desorption to form products are now given by the following two steps.



Again, step three is taken to be rate controlling and essentially irreversible. The rate equation for carbon monoxide becomes

$$r_{CO} = k_3 c_{COS_1} c_{HS_2} \quad (B.15)$$

The concentrations of molecular carbon monoxide and atomic hydrogen on the catalyst surface are again solved for using the first two steps of the mechanism.

$$c_{COS_1} = K_{CO} P_{CO} c_{S_1} \quad (B.16)$$

$$c_{HS_2} = \sqrt{K_{H_2} P_{H_2}} c_{S_2} \quad (B.17)$$

When Equations (B.16) and (B.17) are substituted into Equation (B.15) the following expression results.

$$r_{CO} = k_3 K_{CO} \sqrt{K_{H_2} P_{H_2}} P_{CO}^{0.5} c_{S_1} c_{S_2} \quad (B.18)$$

The concentration of surface sites are again solved for by using total site balances.

$$c_{T_1} = c_{S_1} + c_{COS_1} + c_{CHOS_1} + c_{CH_2OS_1} + \sum_{i=2}^n c_{I_i S_1} + \sum_{i=2}^n c_{I'_i S_1} + c_{CO_2 S_1} \quad (B.19)$$

$$c_{T_2} = c_{S_2} + c_{HS_2} \quad (B.20)$$

Again, carbon dioxide is assumed to be the most abundant surface intermediate. The total site balances can be reduced to the following expressions.

$$c_{T_1} = c_{S_1} + K_{CO_2} p_{CO_2} c_{S_1} \quad (B.21)$$

$$c_{T_2} = c_{S_2} \quad (B.22)$$

When Equations (B.21) and (B.22) are solved for their respective free surface site concentrations and substituted into Equation (B.18) the result is

$$r_{CO} = \frac{k_p p_{CO} p_{H_2}^{0.5}}{(1 + K_{CO_2} p_{CO_2})} \quad (B.23)$$

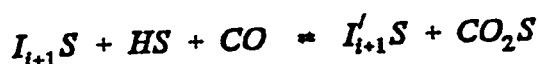
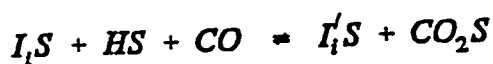
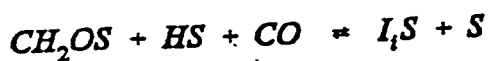
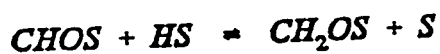
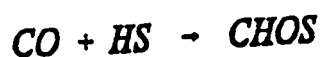
where

$$k_p = k_3 K_{CO} \sqrt{K_{H_2}} c_{T_1} c_{T_2} \quad (B.24)$$

This mechanism leads to a final expression in which the denominator is first order ($c=1$ from empirical fit).

Rideal mechanism, H₂ adsorbed

In this mechanism H₂ is dissociatively adsorbed and carbon monoxide reacts with the adsorbed hydrogen from the gas phase. The reaction can be represented by the following seven steps.



For the Rideal mechanism, the desorption to form products are given by the following two steps.



The reaction between adsorbed hydrogen and gas phase carbon monoxide is assumed to be the rate-determining and essentially irreversible step. Using this assumption, the rate equation is written as follows.

$$r_{CO} = k_2 p_{CO} c_{HS} \quad (B.25)$$

When c_{HS} is solved for using the first step of the Rideal mechanism and CO_2 is assumed to be the most abundant surface intermediate (for the site balance), the rate equation for carbon monoxide becomes

$$r_{CO} = \frac{k_p p_{CO} p_{H_2}^{0.5}}{(1 + K_{CO_2} p_{CO_2})} \quad (B.26)$$

where

$$k_p = k_2 \sqrt{K_{H_2}} c_T \quad (B.27)$$

The Rideal mechanism also leads to a final expression in which the denominator is first order.

Discrimination Between Mechanisms

As shown in the previous section, mechanisms can be written that result in a final

form of the carbon monoxide rate equation with c equal to either 1 or 2. Carbon monoxide is either molecularly adsorbed or reacts from the gas phase. Hydrogen is dissociatively adsorbed in all cases. The rate-determining step in all three mechanisms assumes that initiation is the slow step, while propagation occurs fairly rapidly. This would lead to a product distribution that is constant with CO conversion. In this study, the product distribution did remain fairly constant with CO conversion. Runs over the 7% Ce-ZrO₂ catalyst covered the CO conversion range from 13-35% while the product distribution (wt%) remained at approximately 30% C₁, 8% C₂, 6% C₃, 29% C₄, and 27% C₅+

The assumption that carbon dioxide is the most abundant (most strongly adsorbed) surface species is reasonable. The poor fit found when CO inhibition was used supports the assumption that CO was not a major surface specie. As mentioned earlier, however, rejection of the $c=1$ or $c=2$ model was not possible with the data collected in this study. Perhaps data at higher conversions or conversion data when carbon dioxide is included in the feed would help in the model selection process.

TABLE B.1. Comparison of fitted parameters obtained from SimuSolv[®] for different c values for 7% Ce-ZrO₂ at 50 atm and 1/1 CO/(H₂+H₂S) ratio

T(K)	$c=1$		$c=2$	
	$k_p \times 10^6$ $\left(\frac{\text{mol}}{\text{kg}_{\text{cat}} \text{ atm}^{1.5} \text{ sec}}\right)$	K_{CO_2} (atm^{-1})	$k_p \times 10^6$ $\left(\frac{\text{mol}}{\text{kg}_{\text{cat}} \text{ atm}^{1.5} \text{ sec}}\right)$	K_{CO_2} (atm^{-1})
648	4.73	0.804	4.80	0.335
673	10.97	0.503	12.85	0.252
698	14.85	0.350	17.38	0.170
723	20.55	0.255	24.23	0.125

TABLE B.2. Changes in activation energy and CO₂ heat of adsorption with c for 7% Ce-ZrO₂ at 50 atm and 1/1 CO/(H₂+H₂S) ratio

c	E_a (kcal/mol) ^a	$\Delta H_{\text{ads}} \text{ CO}_2$ (kcal/mol)
1	12.14 ± 0.50	14.22 ± 0.58
2	12.25 ± 0.59	12.50 ± 0.67

^a To convert to kJ/mol multiply by 4.184

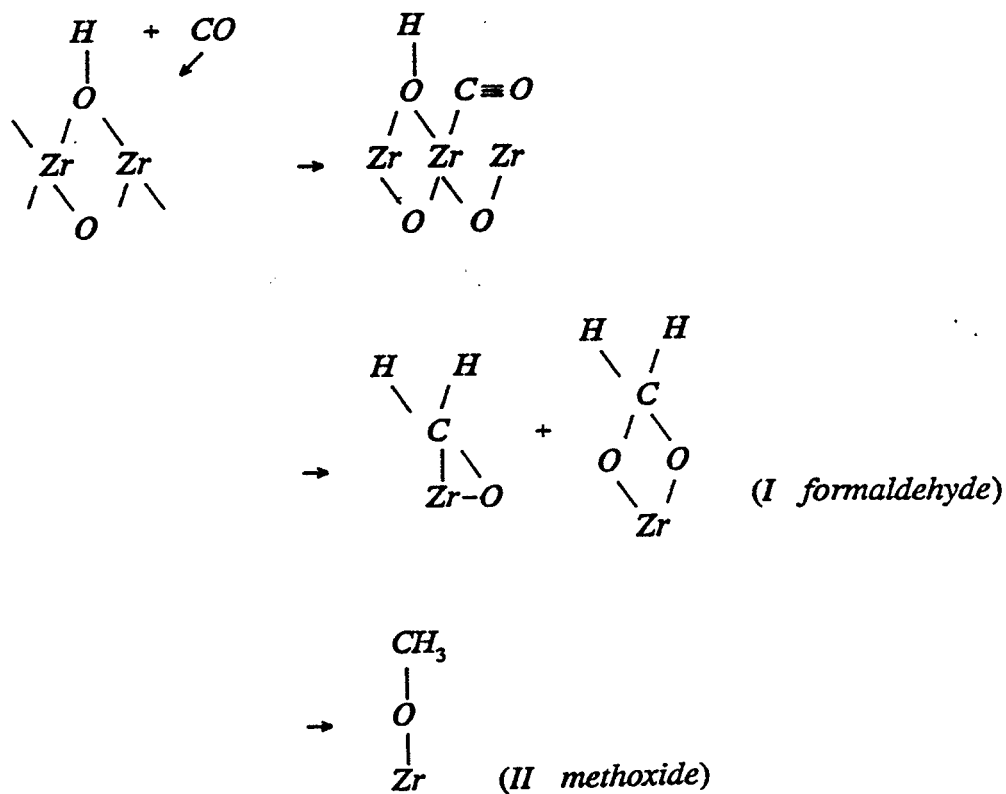


Figure B.1. Formation of adsorbed formaldehyde and methoxide species. Adapted from ref. (15,51).

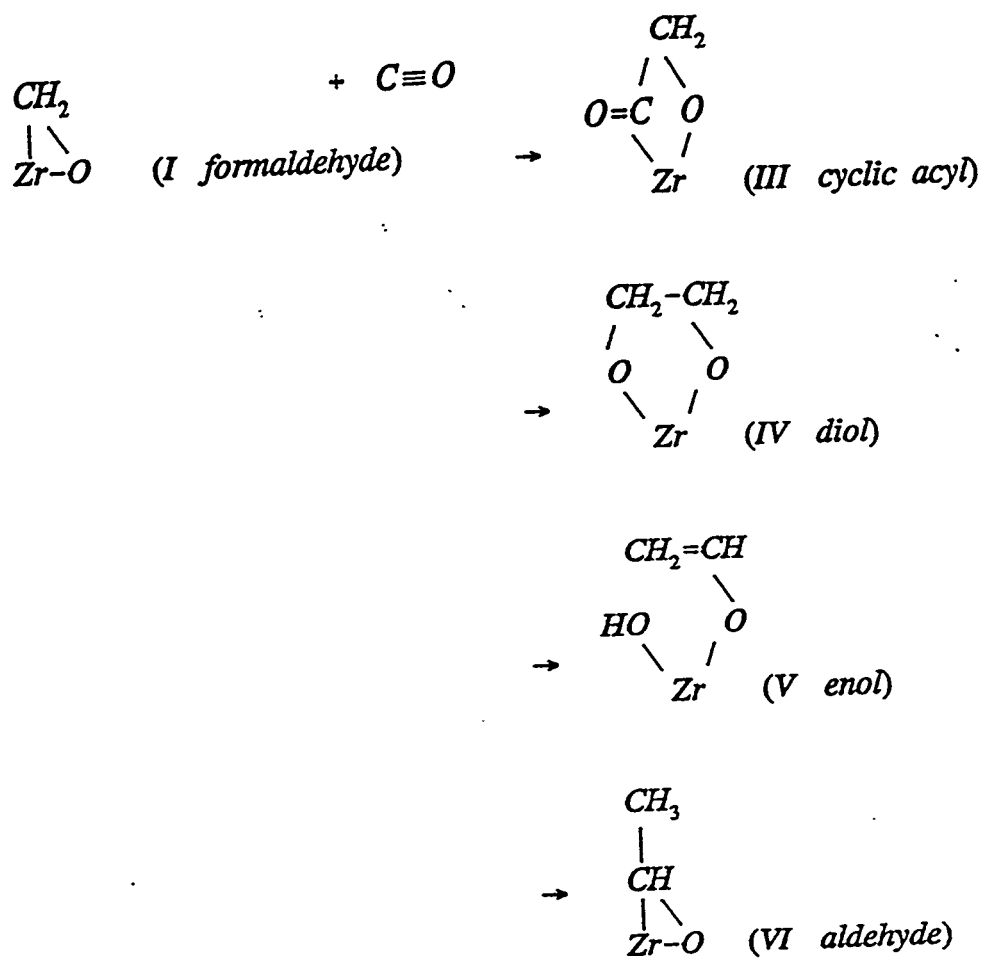


Figure B.2. Mechanism of chain propagation via CO insertion. Adapted from ref. (15).

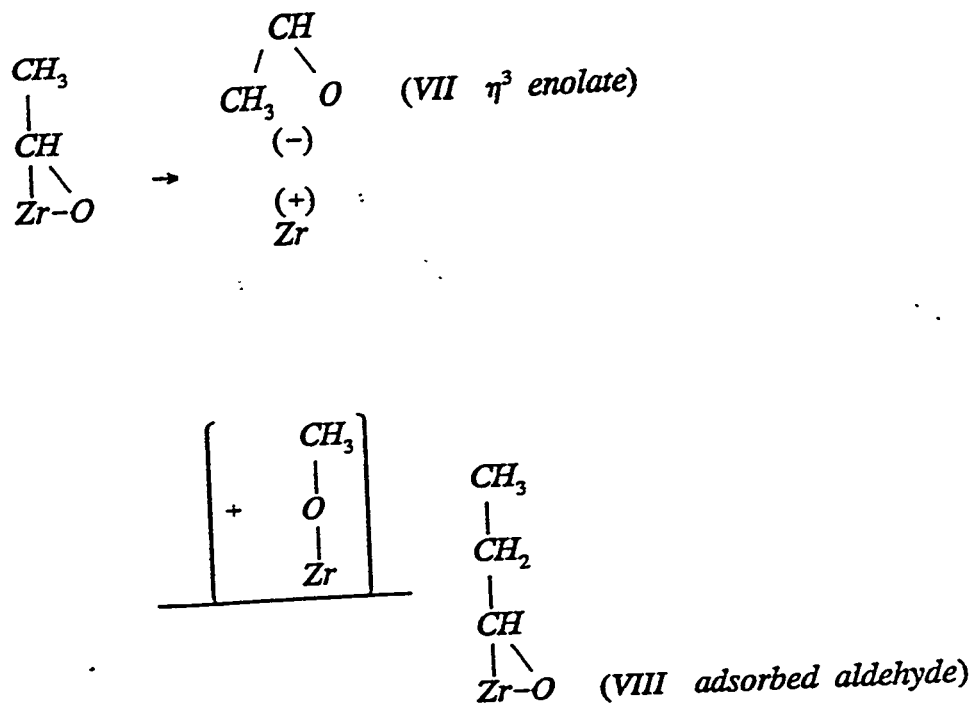
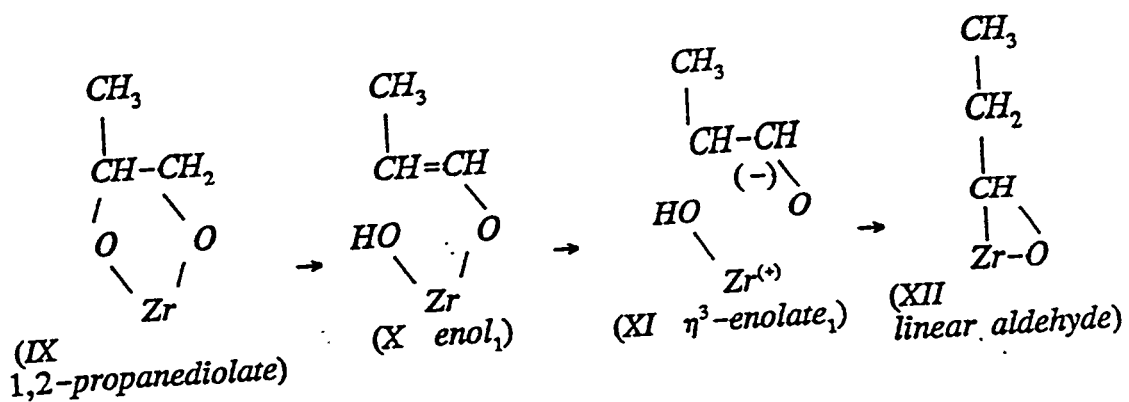


Figure B.3. Mechanism of chain propagation via condensation reaction. Adapted from ref. (15,38)



or:

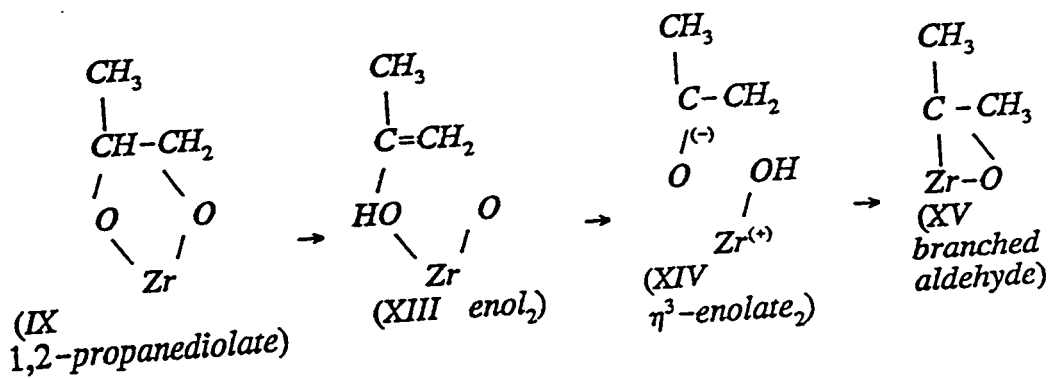


Figure B.4. Formation of linear and branched intermediates. Adapted from ref (15).